

Noise and Vibration Damping with Latex Interpenetrating Polymer Networks

J. A. GRATES, D. A. THOMAS, E. C. HICKEY, and L. H. SPERLING,
*Materials Research Center, Lehigh University,
Bethlehem, Pennsylvania, 18015*

Synopsis

Damping systems based on interpenetrating polymer networks (IPN's) provide noise and vibration attenuation over broad temperature and frequency ranges. Semicompatible latex IPN's are employed in both extensional and constrained layer configurations. The damping behavior of IPN's of compositions poly(ethyl methacrylate)/poly(*n*-butyl acrylate) [PEMA/*Pn*BA], poly(ethyl methacrylate-co-ethyl acrylate)/poly(*n*-butyl acrylate-co-ethyl acrylate) [P(EMA-co-EA)/P(*n*BA-co-EA)], and poly(vinyl chloride)/poly(butadiene-co-acrylonitrile) [PVC/P(B-co-AN)] were investigated and compared to both commercially available materials and to theory. The damping of both the PEMA/*Pn*BA and the P(EMA-co-EA)/P(*n*BA-co-EA) IPN's in a constrained layer configuration was significantly better, over a broad temperature range of -10° to 60° C, than the commercial materials. In addition, the P(EMA-co-EA)/P(*n*BA-co-EA) IPN was found to be effective in damping phenolic-impregnated Kevlar cloth laminates. A reduction of 10 dB in impact noise resulted with a 6-8% by weight layer inserted between the Kevlar-phenolic panels. The relationship between the peak damping temperature of a constrained layer system to maximum $\tan \delta$ along with that of an extensional damping system to maximum E'' was also demonstrated. Although the amount of damping predicted by the theory approached that found experimentally, sufficient differences existed such that the exact detail of the damping curve was not described.

INTRODUCTION

When polymers are in their glass transition region, the time required to complete an average coordinated movement of the chain segments approximates the length of time of the measurement. When dynamic or cyclical mechanical motions are involved, the time required to complete one cycle, or its inverse, the frequency is the time unit of interest. At the glass transition conditions, which involve both temperature and frequency effects, the conversion or degradation of mechanical energy to heat reaches its maximum value. The degradation of vibrational energy to heat is of special interest in damping unwanted noise because a polymer, at its glass transition conditions and in contact with a vibrating surface, rapidly converts the mechanical energy to thermal energy, thereby reducing the emitted noise.

An increased awareness of the effects of unwanted noise has resulted in a heightened interest in the field of noise reduction with concomitant evolution of legislation in the United States and elsewhere. It is possible to reduce noise by absorption, as with acoustical tiles; by a physical barrier; or by damping at the

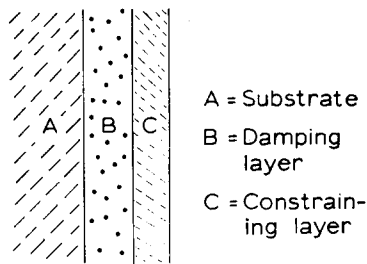


Fig. 1. Constrained layer damping configuration.

source.¹ This paper will be primarily interested in materials used in coating systems for vibration damping at the source.

The theoretical aspects of resonant vibration attenuation by coatings have been described by Ungar,² who described two main types of coating configurations: extensional and constrained. An extensional damping treatment is a single-layer coating in which energy dissipation (and consequent damping) evolves primarily from the flexural and extensional motions of the damping layer. A constrained layer treatment, Figure 1, consists of a two-layer system with a viscoelastic layer under a stiff constraining layer. The addition of the constraining layer produces a shearing action within the viscoelastic layer as the composite panel vibrates. The shear action in combination with flexure and extension greatly increases the amount of energy dissipated per cycle over extensional systems.

The extensional damping coating and the viscoelastic layer of the constrained system are based on polymeric materials which are selected because of their relatively high loss factors under the required conditions. The temperature and frequency sensitivity of polymeric materials with respect to their loss factor and elastic modulus is well known. The width of the glass transition region defines the useful damping range of the polymer. For homopolymers and random copolymers, the useful damping range is approximately 20° to 30°C.³⁻⁵ Acoustical frequencies of interest span the range of 20 Hz to 20,000 Hz, three decades. For many polymers, the time-temperature equivalence is 6° or 7°C per decade of frequency, or about 20°C for the acoustical range. Thus, a homopolymer will just damp the full acoustical range at one temperature. However, many noisy or vibrating systems (machinery, outdoor needs) have their temperature varied by external conditions.

Materials consisting of incompatible (nonmiscible) polymer blends or grafts with widely separated transition temperatures will have two regions of high damping separated by an intermediate region of low damping.⁶⁻⁸ Semicompatible polymer blends and grafts which have extensive but incomplete molecular mixing, on the other hand, have a rather broad region of high damping which may span the range between the two transitions.^{9,10} An important way to control molecular mixing in graft copolymers is by crosslinking both polymers. When the number of deliberately introduced crosslinks in both polymers outnumber the accidentally introduced grafts, a new mode of controlling phase morphology results. These materials are known as interpenetrating polymer networks (IPN's).¹¹⁻²⁰ IPN's are synthesized by swelling a crosslinked polymer (I) with a second monomer (II), plus crosslinking and activating agents and

polymerizing II in situ.^{21,22} By selecting IPN's of specific composition, a number of damping materials having broad but controlled, useful temperature ranges of damping have been synthesized, and have been incorporated into a constrained-layer damping system.²³⁻²⁶ These damping materials were conceived as a broad-temperature damping system which could easily be coated onto a wide variety of substrate configurations by dipping, spraying, or brushing. The present study was concerned with refinements of this basic system. Improved materials for use as the viscoelastic damping layer were sought, and attention was centered on materials having optimum damping properties in the vicinity of room temperature.

The effectiveness of the constraining layer depends directly on its modulus for plastic materials. Several composite systems were formed and investigated, involving both particulate and fibrous fillers. The damping properties of these materials were compared to each other and to commercial materials over a broad temperature range (-30° to 60°C).

Engineering studies were also conducted on the effect of the thickness ratio of constraining layer to viscoelastic layer. In addition, equations from the literature were employed to compare theory with experiment, with the aid of computer programming.

EXPERIMENTAL

Materials

The IPN's used in this work were synthesized by emulsion polymerization techniques described elsewhere. Formula A is a latex 25/75 poly(ethyl methacrylate)/poly(*n*-butyl acrylate) [PEMA/P*n*BA] IPN which had been used in the prototype I formulation.²³ Formula G consisted of a (9-co-21)/(21-co-49) poly(ethyl methacrylate)/poly(*n*-butyl acrylate) [P(EMA-co-EA)/P(*n*BA-co-EA)] latex IPN.²⁴ Prototype II employs formula G as the viscoelastic layer. Formula K, a high-temperature material, was emulsion polymerized under pressure with composition 50/(34-co-16) poly(vinyl chloride)/poly(butadiene-co-acrylonitrile) [PVC/P(P(B-co-An))]. In all cases, the first-mentioned polymer formed the seed latex.

The damping properties of two random copolymers were also explored. These were a latex 55-45 random copolymer of ethyl acrylate and methyl methacrylate, formula H, and a 70/30 EA/MMA latex random copolymer, formula J, both also prepared by emulsion polymerization. The former was designed as a room-temperature optimized extensional damper, while the latter was intended as the viscoelastic layer in a constrained layer system also optimized for room temperature. Several commercial extensional damping materials were compared to our materials. Two of these, B and C, were highly filled coatings based on poly(vinyl acetate). The rest, D, E, and F, were of unknown composition. The several materials employed are described in Table I.

The efficacy of various materials as constraining layers was also investigated (Table II). A highly filled epoxy, HS 7130 (High Strength Plastics, Chicago, Ill.), reinforced with 5% by weight Fybex (E. I. du Pont de Nemours & Co., Inc., Wilmington, Del.), M, was used in this study. Epon 828 (Shell Chemical Corp.) was used as a constraining layer both by itself, P, and reinforced with fiber glass. Two types of fiber glass were used, a 9-mil-thick mat of randomly distributed

TABLE I
Composition of Damping Polymers

Designation	Source	Composition
A	IPN	75/25 poly(ethyl methacrylate)/poly(<i>n</i> -butyl acrylate)
B	commercial	poly(vinyl acetate)
C	commercial	poly(vinyl acetate)
D	commercial	unknown
E	commercial	unknown
F	commercial	unknown
G	IPN	(9-co-21)/(21-co-49) poly(ethyl methacrylate-co-ethyl acrylate)/poly(<i>n</i> -butyl acrylate-co-ethyl acrylate)
H	random copolymer	55/45 ethyl acrylate/methyl methacrylate
J	random copolymer	70/30 ethyl acrylate/methyl methacrylate
K	IPN	50/(30-co-16) poly(vinyl chloride)/poly(butadiene-co-acrylonitrile)

TABLE II
Composition of Constraining Layers

Designation	Composition
M	HS7130 reinforced with 5% Fybex
N	15 mil aluminum
P	Epon 828
Q	Epon 828 reinforced with fiber glass mat
R	Epon 828 reinforced with fiber glass cloth
S	13.5 mil steel
T	Laminate of Kevlar fabric impregnated with phenolic

glass fibers, Q, and a 3-mil-thick woven glass cloth, R, having the same weight per unit area as the glass mat. Stiffer constraining layers of 15 mil aluminum, N, and 13.5 mil steel, S, were also studied. A further set of experiments was carried out using phenolic impregnated Kevlar cloth laminates, T, in sandwich form, where the Kevlar materials served as both substrate and constraining layer. Each laminate consisted of 20 layers, 10 layers on each side, producing a material approximately 1.5 cm thick. Several thicknesses of damping latex IPN were incorporated in sandwich form.

Coating Procedures

The reeds used in these experiments were cut from Nicholson precision ground type 01 tool steel and measured $\frac{1}{2}$ in. \times 8 in. \times 62.5 mils thick. The various materials of interest were coated onto one side of the reeds, the total thickness of the coating equaling the 62.5-mil substrate thickness. Except in cases where the thickness ratio was intentionally varied, the thickness of the constraining layer equaled the thickness of the viscoelastic layer at 31.25 mil each.

In a separate experiment, steel panels 1 ft \times 5 in. \times 62.5 mils in size were coated with the materials of interest. Again, the total coating thickness was approximately equal to the substrate thickness, and constraining and viscoelastic layer thicknesses were equal. The coated panels were suspended with thin wires inside a small acoustically treated chamber designed in this laboratory.

A General Radio Model 1565B sound meter, set in the fast mode with an A weighting, was positioned directly above the panel to measure impact noise. As the panel was struck by a hard plastic ball, the peak reading in dBA was recorded. Since acoustical measurements at several temperatures were of interest, the panels were cooled or heated before being tested to provide for temperature control.

In a separate paper,²⁴ the loss modulus E'' , the storage modulus E' , and the loss tangent $\tan \delta$, which is equivalent to the ratio E''/E' , were determined for the damping materials. The results will be summarized here, as necessary. Studies were conducted over the temperature range of interest at a frequency of 110 Hz.

Comparison to Theory

Using Ungar's² theoretical approach to constrained layer damping, a computer program was written to calculate the per cent critical damping of composite panels or reeds. The program incorporated as parameters the densities and thicknesses of the substrate and of both layers; the elastic modulus of the substrate and constraining layer; the frequency; and the storage modulus and loss tangent of the viscoelastic layer. The equations employed are defined in Appendix I. With this program it was possible to predict the effects that different temperatures and thickness ratios would have upon the composite damping.

Instrumentation

Several experiments were employed to determine the damping properties of the various materials.

A vibrating reed apparatus employing a Model SD-A vibrator (MB Manufacturing Co., New Haven, Conn.) was driven by a Hewlett-Packard Model 2020 low-frequency oscillator. A Wilcoxon Model 111 accelerometer (Wilcoxon Research, Bethesda, Md.) was attached to one end of the reed, and the output was fed to a Tektronix Model 315 D oscilloscope (Tektronix, Inc., Portland, Or.). To obtain better resonance performance, a counterweight equal to the accelerometer was placed at the other end of the reed. The oscilloscope was triggered to provide a single horizontal sweep as the excitation force to the reed was cut off. The resulting waveform, a decaying sinusoid, was photographed with a 35-mm camera and the photograph was used to determine the composite damping.

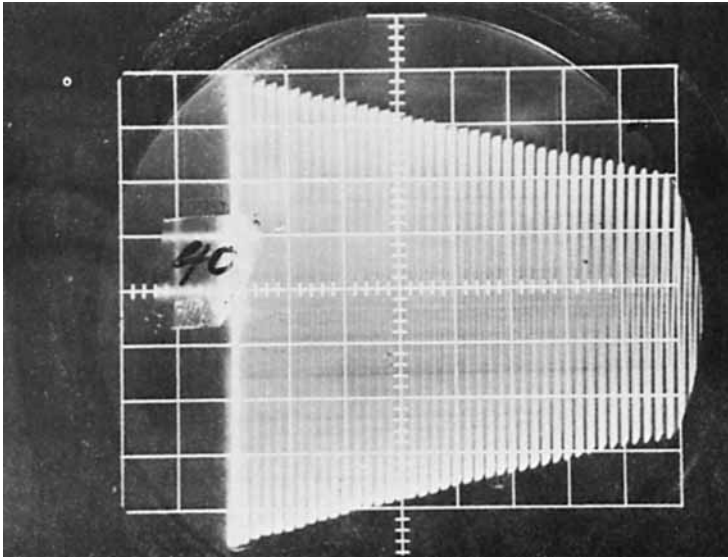
By measuring the vibrational decay rate, it is possible to determine the logarithmic decrement Δ , and from this the per cent critical damping. Thus,

$$\Delta = -\frac{1}{N} \ln \frac{\chi_N}{\chi_0} \quad (1)$$

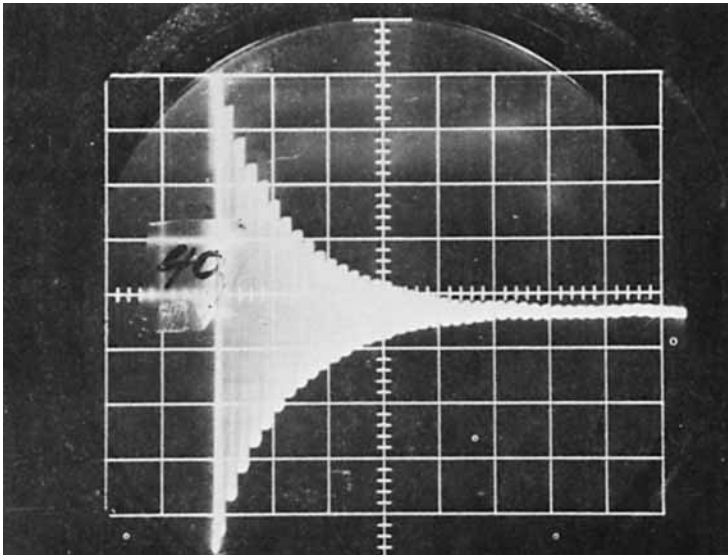
where Δ = logarithmic decrement, N = number of cycles, χ_0 = initial amplitude, and χ_N = amplitude after N cycles. From the logarithmic decrement, it is possible to calculate the per cent critical damping using the relation

$$\% \text{ C.D.} = 100(2\pi\Delta). \quad (2)$$

Examples of the waveforms generated by a highly damped and an undamped reed are depicted in Figure 2. An example of the waveform generated by an



(a)



(b)

Fig. 2. Oscilloscope traces of vibration decay: (a) undamped reed; (b) highly damped reed.

undamped reed is shown in Figure 2a, and a reed damped with formula G with constraining layer M is shown in Figure 2b.

Experiments with the vibrating reed apparatus were carried out at a resonant frequency of approximately 600 Hz, the exact frequency being dependent upon the resonance point of the particular reed in use. Temperature variation was made possible by inserting the reed into an environmental chamber and cooling with liquid nitrogen. An internal heater was employed to control the temperature rise at a rate between 1° and 2°C per min.

RESULTS

Figure 3 compares prototype I (formula A constrained with M) with various commercial materials over a broad temperature spectrum. Whereas the commercial materials, B, C, D, E, and F, all tend to peak sharply at one temperature, A shows relatively high damping throughout the temperature range. Although formula A provides a good broad-temperature damping system, the damping undergoes a slight minimum at room temperature. Consequently, formula G was synthesized²⁴ to provide optimum damping characteristics in the room-temperature region, as well as for significant high and low temperature utility.

Figure 4 demonstrates the damping capabilities of formula G in both extensional and constrained layer modes as a function of temperature. In the latter mode, the constraining layer material M was employed. Formula G shows a superiority to the damping properties of formula A in the region of -20°C to $+50^{\circ}\text{C}$, the range of greatest interest.

Ball and Salyer^{27,28} and Ungar² have noted that E'' is of greatest importance in extensional damping, whereas the value of $\tan \delta$ is of greatest importance in constrained layer treatments. This dependence is clearly evident when comparing the vibrating reed data of Figure 4 with the dynamic mechanical spectroscopy data of Figure 5. There is a very close correspondence between the E''

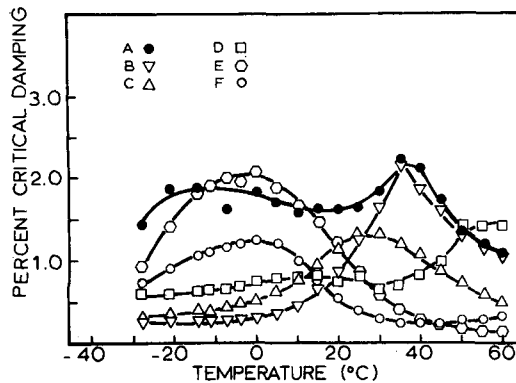


Fig. 3. Temperature dependence of damping for formula A and commercial materials.

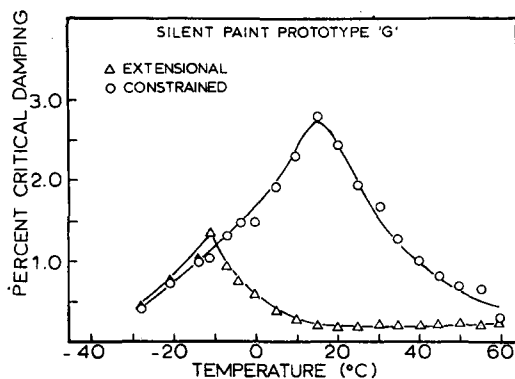


Fig. 4. Extensional and constrained layer damping of formula G as a function of temperature.

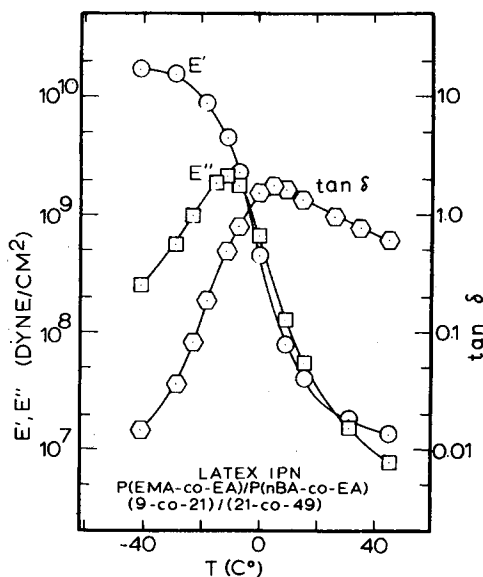


Fig. 5. Storage modulus E' , loss modulus E'' , and $\tan \delta$ values for formula G.

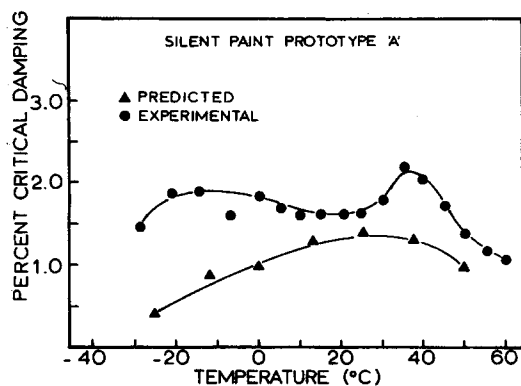


Fig. 6. Comparison of theoretical and experimental constrained layer damping for formula A as a function of temperature.

peak at -11°C in Figure 5 and the extensional damping peak at -10°C in Figure 4. In addition, the $\tan \delta$ peak at 6°C also corresponds to the constrained layer damping peak at 15°C . The slight variation in temperatures can be ascribed to experimental error and the differences in frequencies employed (DMS at 110 Hz, vibrating reeds at 600 Hz).

Figure 6 compares the temperature dependence of formula A from Figure 3 with theory. The predicted damping curve provides a reasonably close approximation to the actual damping curve, but predicts the damping to be lower than found by approximately a factor of 2. Also, the details of the curve, especially the shallow minimum near room temperature, are not reproduced by the theory.

An attempt was made to study the effective damping as a function of the constraining layer-to-viscoelastic layer thickness ratio. Reeds were prepared with the constraining layer thickness fraction ranging from 0 (all viscoelastic

TABLE III
Constrained Layer Damping at 28°C

Viscoelastic layer	Constraining layer	Critical damping, %
J	M	2.27
G	M	1.90
A	M	1.70
A	N	1.39
K	M	1.02
A	R	0.78
A	Q	0.76
A	P	0.63

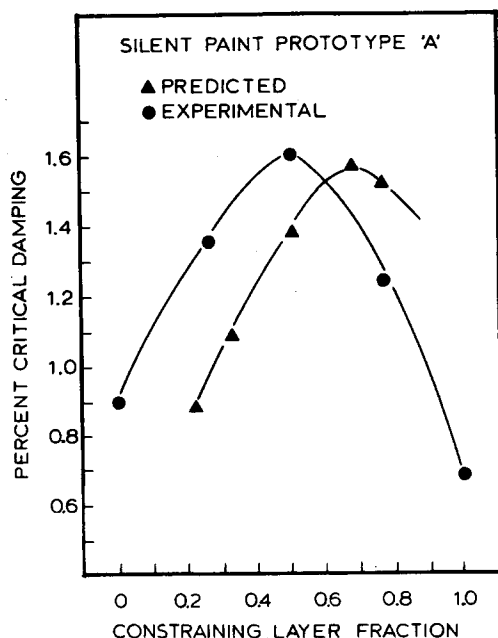


Fig. 7. Comparison of theoretical and experimental constrained layer damping as a function of the ratio of constraining layer thickness to viscoelastic layer thickness.

layer) to 1 (all constraining layer). Formula A was used as the viscoelastic layer constrained with material M. The results are shown in Figure 7. The experiments, all performed at 25°C, indicate a maximum near the 50/50 ratio. A computer simulation was also performed using Ungar's theory,² which indicated a damping maximum near the 70/30 constraining layer-to-viscoelastic layer ratio. Thus, the theory, which is an approximation, usefully describes the data in broad outline but not in detail.

Table III ranks the damping ability of the various constrained layer materials at 28°C. The 70/30 EA/MMA random copolymer, J, in a constrained layer configuration was found to have the greatest damping. This was followed closely by prototype II and prototype I latex IPN'S. The effect of constraining layer stiffness is clearly shown in this table. On separate reeds, formula A was constrained with Fybex-reinforced HS 7130, aluminum foil, and Epon 828 (reinforced and not reinforced). Although the aluminum foil is the stiffest of the three

TABLE IV
Extensional Damping at 28°C

Damping layer	Critical damping, %
B	1.60
C	1.25
H	1.23
J	0.70
M	0.69
D	0.60
F	0.50
K	0.34
E	0.30
G	0.26
Bare reed	0.24

TABLE V
Impact Noise Data

Viscoelastic layer	Constraining layer	Noise level, dBA		
		-10°C	22°C	60°C
Bare steel panel	—	97.5	100	97
E	—	75	73	83
B	—	87	77	74
G	M	77	74	77
G	S	75.5	73	79
D	—	88.5	77	79
A	M	74	75	75
A	S	72.5	73.5	75
A	R	73.5	75	74.5
C	—	87	75	74

types, the reed constrained with it falls somewhat below that reed constrained with HS 7130. This is due to the fact that the foil has only half the thickness of the other constraining layers. Epon 828 is a somewhat flexible epoxy, and consequently lower damping results. As would be expected, the damping of the glass cloth-reinforced Epon 828 is better than that with the glass mat due to the greater packing density of the glass cloth. Both of these compositions are much better than the reed constrained with Epon 828 alone.

Table IV illustrates the damping capabilities of the various materials in the extensional mode at 28°C. The commercial materials, B and C, both based on poly(vinyl acetate), provide the best damping capability. However, comparison of data in Table IV with those in Table III illustrates the superiority of the constrained layer damping systems.

Table V shows the results of the acoustically treated chamber test at three temperatures. These results confirm the data found in the vibrating reed experiments measuring the actual noise generated. Here, formula G constrained with a thin steel layer, S, was found to be superior at room temperature. Again, the stiffness of the constraining layer was found to have a direct relationship on the effectiveness of the damping treatment. The high temperature sensitivity of the commercial materials is contrasted with the lower sensitivity of formula G and the relative temperature insensitivity of formula A. The panels used for this test consisted of a steel substrate.

TABLE VI
Kelvar Panel Impact Noise Data

Weight, % G	Noise level, dBA		
	4°C	29°C	50°C
0	82.7	81.7	72.2
6.0	73.7	71.3	66.8
8.2	73.7	70.2	66.2
12.5	72.2	70.0	66.5

Separately, panels consisting of phenolic impregnated Kevlar cloth laminates, in sandwich form were tested in the chamber. Several thicknesses of formula G were used as the viscoelastic layers in these panels. Table VI presents the impact noise level of the panel at 4°, 29°, and 50°C. It is apparent that only a small amount of damping material is needed to provide a significant decrease in the impact noise. The laminate itself appears to undergo transition beginning about 50°C and becomes much more acoustically dead. This could account for the reduced efficiency of the damping material at the highest temperature. Also, formula G has its maximum $\tan \delta$ value slightly below room temperature and has a lower efficiency at 50°C.

DISCUSSION

When the phase domains are very small, of the order of 100 Å in dimension,¹² the classical concept of a sharp boundary dividing two phases breaks down. In fact, the phase dimensions may be smaller than the end-to-end distances normally encountered in polymer molecules,²⁹ 500–800 Å, reinforcing the view that the compositional makeup of 100-Å domains is nonclassical and may vary from point to point. Thus, extensive but incomplete mixing takes place, with each local volume element contributing to the glass transition region according to its composition. Depending upon the exact degree of phase separation, the transition may be broader or narrower. The limit of complete molecular mixing produces narrow transitions resembling random copolymers,^{9,10} while the limit of gross incompatibility produces two sharp transitions, each one representative of its own homopolymer.

Latex IPN formulations A and G represent different broad-temperature damping systems. Formulation A has only poly(ethyl methacrylate) and poly(*n*-butyl acrylate) in polymers I and II, respectively. The $\tan \delta$ values are nearly constant with temperature, but actually exhibit a slight minimum between the two transitions. Formulation G has a common comonomer, ethyl acrylate, incorporated in both polymer I and polymer II. As a consequence, the $\tan \delta$ -temperature plot of formulation G, Figure 5, is significantly narrower, with a single, well-defined maximum. From an acoustical damping point of view, formulation G was engineered to give the best damping near room temperature (it actually peaks slightly below room temperature at 600 Hz) while retaining significant damping capability over a broad temperature range.

It is of special interest to note that while Ungar's² theory correctly shows that E'' controls extensional damping and $\tan \delta$ controls constrained layer damping (see Figs. 4 and 5), the quantitative aspects of the theory contain some important assumptions, causing a difference in predicted versus experimental results

(Figs. 6 and 7). For example, the damping capability of the constrained layer, acting as an extensional damper on top of the damping layer, is not fully considered. Thus, the experimental value of the percent critical damping is higher than predicted.

This work confirms the theoretical prediction that the per cent critical damping depends upon the stiffness of the constraining layer. Also, sandwich configurations, where the damping material lies between two equal thickness layers, both outer layers serving dually as substrate/constraining portions, is confirmed as a very effective arrangement. Also, since most work reported in the literature has either or both layers metallic,^{2,27,28} Table VI shows that stiff plastics can also be effectively damped.

Appendix I

An iterative procedure was used to calculate the theoretical constrained layer damping of a given treatment using the following equations²:

$$Y = \frac{E_1 H_1^3 + E_3 H_3^3}{12 H_{31}^3} \left(\frac{1}{E_1 H_1} + \frac{1}{E_3 H_3} \right) \quad (1)$$

$$\chi_{\text{opt}} = \frac{1}{\sqrt{(1 + Y)(1 + \beta_2^2)}} \quad (2)$$

$$\bar{B} = (B_1 + B_3) \left(1 + \frac{\bar{\chi} Y}{1 + \bar{\chi}} \right) \quad (3)$$

$$\frac{1}{p^2} = \frac{1}{w} \sqrt{\frac{\bar{B}}{N}} \quad (4)$$

$$\chi = \frac{G_2}{p^2 H_2} \left(\frac{1}{E_1 H_1} + \frac{1}{E_3 H_3} \right) \quad (5)$$

$$N = \frac{(2 + y)\chi_{\text{opt}}}{2} \quad (6)$$

$$\eta_{\text{max}} = \frac{\beta_2 Y}{2 + y + \frac{2}{\chi_{\text{opt}}}} \quad (7)$$

$$\eta = \left[\frac{2(1 + N) \frac{\chi}{\chi_{\text{opt}}}}{1 + 2N \frac{\chi}{\chi_{\text{opt}}} + \left(\frac{\chi}{\chi_{\text{opt}}} \right)^2} \right] \eta_{\text{max}} \quad (8)$$

where Y = stiffness parameter, χ = shear parameter, η = composite loss factor, E = modulus of elasticity, H = thickness of layer, H_{31} = distance between neutral planes of layers = $H_2 + \frac{H_1 + H_3}{2}$, G = real part of complex shear modulus, p = wavenumber, β = shear loss factor,

\bar{B} = complex flexural rigidity, and $B = EH^3/12$ = flexural rigidity of layer; subscripts: 1 = base layer, 2 = viscoelastic layer, 3 = constraining layer, and opt = optimal.

Procedure

1. Calculate stiffness parameter Y for given configuration using eq. (1).
2. Calculate χ_{opt} from eq. (2).
3. Let $\bar{\chi} \approx \chi_{\text{opt}}$ and solve for \bar{B} using eq. (3).
4. From eq. (4), calculate $1/p^2$.
5. Finding χ using eq. (5).

6. Compare this value to the previously used value. If difference is small, stop. If not, use this new value in eq. (3) to find \bar{E} .
7. Repeat steps 4 to 6 until values of χ converge.
8. Calculate N and η_{\max} from eqs. (6) and (7).
9. Use the final value of χ in eq. (8) to find η .
10. To find per cent critical damping, multiply η by 50.

The authors are indebted to the Human Engineering Laboratory of Aberdeen Proving Ground, Aberdeen, Maryland, for financial assistance through contract DAADO5-72-C-0175.

References

1. S. Ikeda, *Progr. Org. Coatings*, **1**, 205 (1972/73).
2. E. E. Ungar, in *Noise and Vibration Control*, L. L. Beranek, Ed., McGraw-Hill, New York, 1971, Chap. 14.
3. D. J. Williams, *Polymer Science and Engineering*, Prentice-Hall, Englewood Cliffs, N.J., 1971.
4. F. Rodriguez, *Principles of Polymer Systems*, McGraw-Hill, New York, 1970.
5. J. H. Aklonis, W. J. MacKnight, and M. Shen, *Introduction to Polymer Viscoelasticity*, Wiley-Interscience, New York, 1972.
6. G. E. Molau, Ed., *Colloidal and Morphological Behavior of Block and Graft Copolymers*, Plenum, New York, 1971.
7. N. A. J. Platzer, *Advan. Chem. Ser.*, No. 99, (1971).
8. H. Keskkula, Ed., *J. Appl. Polym. Sci., Appl. Polym. Symposia*, No. 7, (1968).
9. M. Matsuo, *Jap. Plast.*, **2**, 6 (July 1968).
10. S. Manabe, R. Murakami, and M. Takayanagi, *Mem. Fac. Eng., Kyushu University*, **28**, 295 (1969).
11. L. H. Sperling, V. Huelck, and D. A. Thomas, in *Polymer Networks: Structural and Mechanical Properties*, A. J. Chompff and S. Newman, Eds., Plenum, New York, 1971.
12. V. Huelck, D. A. Thomas, and L. H. Sperling, *Macromolecules*, **5**, 340, 348 (1972).
13. L. H. Sperling and D. W. Friedman, *J. Polym. Sci. A-2*, **7**, 425 (1969).
14. L. H. Sperling, D. W. Taylor, M. L. Kirkpatrick, H. F. George, and D. R. Bardman, *J. Appl. Polym. Sci.*, **14**, 73 (1970).
15. L. H. Sperling, H. F. George, V. Huelck, and D. A. Thomas, *J. Appl. Polym. Sci.*, **14**, 2815 (1970).
16. L. H. Sperling and R. R. Arnst, *J. Appl. Polym. Sci.*, **15**, 2317 (1971).
17. A. J. Curtius, M. J. Covitch, D. A. Thomas, and L. H. Sperling, *Polym. Eng. Sci.*, **12**, 101 (1972).
18. L. H. Sperling and H. D. Sarge, III, *J. Appl. Polym. Sci.*, **16**, 3041 (1972).
19. A. A. Donatelli, D. A. Thomas, and L. H. Sperling, in *Recent Advances in Polymer, Blends, Grafts and Blocks*, Plenum, New York, 1974.
20. L. H. Sperling, R. E. Touhsaent, and D. A. Thomas, presented at Symposium on Recent Advances in Polymer Science, Princeton, N. J., September 1973.
21. L. H. Sperling, T.-W. Chiu, C. P. Hartman, and D. A. Thomas, *Int. J. Polym. Mat.*, **1**, 331 (1972).
22. L. H. Sperling, T.-W. Chiu, and D. A. Thomas, *J. Appl. Polym. Sci.*, **17**, 2443 (1973).
23. L. H. Sperling, T.-W. Chiu, R. G. Gramlich, and D. A. Thomas, *J. Paint Technol.*, **46**, 47 (1974); L. H. Sperling and D. A. Thomas, U.S. Pat. 3,833,404 (1974).
24. L. H. Sperling, J. A. Grates, J. E. Lorenz, and D. A. Thomas, presented at ACS Meeting, Philadelphia, April 1975.
25. L. H. Sperling, D. A. Thomas, J. E. Lorenz, and E. J. Nagel, in preparation.
26. J. A. Grates, J. E. Lorenz, D. A. Thomas, and L. H. Sperling, proceedings International Conference on Noise Control Engineering, 537 (1974).
27. G. L. Ball and I. O. Salyer, *J. Acoust. Soc. Amer.*, **39**, 663 (1966).
28. G. L. Ball and I. O. Salyer, U.S. Pat. 3,399,104 (1968).
29. P. J. Flory, *Principles of Polymer Chemistry*, Cornell University Press, Ithaca, N.Y. 1967.

Received November 4, 1974

Revised November 26, 1974